atoms

MDPI

Article

New Energy Levels and Transitions of $5s^25p^2$ (6d+7s) Configurations in Xe IV

Jorge Reyna Almandos [1,*], Mónica Raineri [1], Cesar J. B. Pagan [2] and Mario Gallardo [1]

[1] Centro de Investigaciones Opticas (CIOp), CC 3, 1897, Gonnet, 1900 La Plata, Argentina; monicar@ciop.unlp.edu.ar (M.R.); mogallardo38@gmail.com (M.G.)

[2] School of Electrical and Computer Engineering, University of Campinas (UNICAMP), 13083-970 Campinas, SP, Brazil; pagan@unicamp.br

* Correspondence: jreyna@ciop.unlp.edu.ar

Received: 17 October 2019; Accepted: 11 December 2019; Published: 17 December 2019

Abstract: Three-times ionized xenon Xe IV spectrum in the 1070–6400 Å region was analyzed using a pulsed discharge light source. A set of 163 transitions was classified for the first time, and 36 new energy levels belonging to the $5s^25p^26d$ and $5s^25p^27s$ even configurations were determined. The relativistic Hartree–Fock method, including core-polarization effects, were used. In these calculations, the electrostatic parameters were optimized by a least-square procedure in order to improve the adjustment to experimental energy levels. We also present a calculation based on a relativistic multiconfigurational Dirac–Fock approach.

Keywords: atomic databases and related topics; astrophysical and laboratory plasmas: atomic data needs; atomic lifetime and oscillator strength determination

1. Introduction

There is great interest in spectroscopy data of Xenon due to their applications in collision physics, astrophysics, and laser physics. Various atomic parameters, such as energy levels, oscillator strengths, transition probabilities, and radiative lifetimes, have many important astrophysical applications. Transition probabilities are needed for calculating the energy transport through the star in model atmospheres [1] and for direct analysis of stellar chemical compositions [2]. Xenon was observed in chemically peculiar stars [3] and planetary nebulae [4]. The spectrum analysis of planetary nebula NGC7027 by Péquignot and Baluteau [5] has stimulated the calculation of transition probabilities for some forbidden lines of astrophysical interest [6]. The Xe VI and Xe VII lines were observed in the ultraviolet spectrum of the hot DO-type white dwarf RE 0503-289 [7,8]. In particular, the Xe IV spectrum was detected in the spectrum of NGC 7027 together with a variety of ionic species, providing a unique opportunity to study the chemical composition of the nebula at a level normally unachievable in another emission line nebulae [9,10].

Saloman [11] published a revised compilation of energy levels and observed spectral lines of all ionization stages of Xe, referring to studies published to date [12–16]. Light sources include direct-current hollow cathode discharge, theta-pinch discharge, and pulsed capillary discharge. Most of the information is from two studies: Tauheed et al. [13] classified 114 Xe IV lines in VUV using a modified triggered spark initiated by a xenon gas blast as spectral source, and Gallardo et al. [14], who analyzed the $5s^25p^26p$, $5s^25p^24f$, $5s5p^4$, $5s^25p^25d$, and $5s^25p^26s$ configurations, providing the wavelengths for 618 classified lines in their list, using a capillary discharge as light source.

More recently the study by Raineri et al. [15] reported the weighted oscillator strengths and cancellation factor (CF), calculated from fitted values of the energy parameters of all 769 dipole electric lines belonging to the Xe IV spectrum reported in the compilation [11], including 49 new classified lines.

Hartree–Fock relativistic (HFR) calculations and parametric fits were used. In addition, the results presented in their study were compared to those from Bertuccelli et al. [16].

In order to proceed withthe study of the threetimes ionized xenon spectrum, a new spectral analysis of this ion is presented in this paper. New 36 energy levels for $5s^25p^2$ (6d+7s) configurations and 163 new transitions in the 1070–6400 Å region are reported. The relativistic Hartree–Fock method based on the code of Cowan [17] was used. The energy matrix was calculated using energy parameters adjusted to fit the experimental energy levels. Core polarization effects were taken into account in our calculations [18]. We also present a multiconfigurational relativistic approach for the Dirac equation (MCDF), by using the general relativistic atomic structure package (GRASP) [19].

2. Experimental Methods

The spectral source used in this study is based on the pulsed discharge tube built at the Centro de Investigaciones Opticas to study highly ionized noble gases [20]. It consists of a Pyrex tube of about 100 cm with inner diameter of 0.5 cm. The electrodes, placed 80 cm apart, are made of tungsten covered with indium to avoid the impurities coming from the electrodes. The gas excitation was produced by discharging a bank of low-inductance capacitors ranging from 20 to 280 nF, charged with voltages up to 20 kV. The VUV region of the spectrum was recorded using a 3m normal incidence spectrograph equipped with 1200 lines/mm concave diffraction grating and with a plate factor of 2.77 Å/mm in the first diffraction order. Internal wavelength standards are from C, N, O, and known lines of xenon. The wavelength range above 2000 Å was recorded using a 3.4 m Ebert plane-grating spectrograph with 600 lines/mm and a plate factor of 5 Å/mm in the first diffraction order. Thorium lines from an electrodeless discharge were superimposed on the spectrograms and served as reference lines. A photoelectric semiautomatic Grant comparator was used to measure the spectrograms. The uncertainty of the wavelength values of lines was estimated to be correct to ±0.01Å above 2000 Å and ±0.02 Å in the VUV region.

3. Results and Discussion

In this study, we used the modified version of Cowan's atomic calculation package [17], described in our paper [18], for the inclusion of the polarization potentials as a modification in the Hartree–Fock equations. In addition, we considered the corrections of the reduced matrix element used in our previous papers [21], which is the same modification used by Quinet et al. [22] to correct transition matrix elements when including CP and core penetration effects. These methods demand knowledge on the polarizability andcore cut-off radius. The value of α_d for Xe IV core, that is, for Xe 8+ is given by Koch [23] in 0.81130 $a_0{}^3$ and the rc value in 1.16 a_0, defines the boundaries of the atomic core.

We adjusted the values of energy parameters to the experimental energy levels of the Xe IV through a least-squares calculation. With the adjusted values, we calculated the composition of the $5s^25p^2$ (6d+7s) energy levels presented in Table 1, where we included lifetimes calculated using HFR and HFR+CP with adjusted energy parameters (here named HFRa and HFR+CPa, respectively) and using multiconfigurational Dirac Fock (MCDF). The MCDF approach was carried out with the extended average level assuming a uniform charge distribution in the nucleus, with a xenon atomic weight of 131.3. The values presented in this work for lifetimes in the MCDF calculation are in Babushkin gauge since this one, in the non-relativistic limits (length), has been found to be the most stable value in many situations, in the sense that it converges smoothly as more correlation is included [24].

Table 1. Energy levels, composition, and lifetimes of Xe IV.

Designation		Energy (cm^{-1})		Composition	Lifetime(ns)		
		Exp.	Fitted		HFRa	HFR +CPa	MCDF Babushkin
$5s^25p^2(^3P)7s$	$^4P_{1/2}$	239,145	239,126	68.8%^{4}P + 22.5% $5s^25p^2(^3P)7s\ ^2$P + 8.1% $5s^25p^2(^1S)7s\ ^2$S	0.304	0.297	0.364
	$^4P_{3/2}$	246,689	246,769	84.5%^{4}P + 9.2% $5s^25p^2(^3P)7s\ ^2$P + 3.3% $5s^25p^2(^3P)6d\ ^4$D	0.324	0.322	0.414
	$^2P_{1/2}$	247,583	247,559	66.7%^{2}P + 23.2% $5s^25p^2(^3P)7s\ ^4$P + 3.8% $5s^25p^2(^3P)6d\ ^2$P	0.247	0.232	0.298
	$^4P_{5/2}$	251,851	251,784	74.6%^{4}P + 22.9% $5s^25p^2(^1D)7s\ ^2$D	0.355	0.357	0.553
	$^2P_{3/2}$	252,943	252,992	62.5%^{2}P + 25.1% $5s^25p^2(^1D)7s\ ^2$D + 6.7% $5s^25p^2(^3P)7s\ ^4$P	0.190	0.190	0.287
$5s^25p^2(^1D)7s$	$^2D_{5/2}$	266,331	266,382	60.5%^{2}D + 17.1% $5s^25p^2(^3P)7s\ ^4$P + 9.6% $5s^25p^2(^1D)6d\ ^2$D	0.239	0.257	0.287
	$^2D_{3/2}$	266,623	266,574	68.9%^{2}D + 22.7% $5s^25p^2(^3P)7s\ ^2$P + 3.6% $5s^25p^2(^3P)7s\ ^4$P	0.221	0.228	0.176
$5s^25p^2(^1S)7s$	$^2S_{1/2}$	283,512	283,519	91.3%^{2}S + 5.2% $5s^25p^2(^3P)7s\ ^4$P + 2.9% $5s^25p^2(^3P)7s\ ^2$P	0.318	0.302	0.454
$5s^25p^2(^3P)6d$	$^4F_{3/2}$	234,291	234,304	58%^{4}F + 15% $5s^25p^2(^3P)6d\ ^4$D + 10% $5s^25p^2(^3P)6d\ ^2$P	0.519	0.563	0.507
	$^4F_{5/2}$	235,660	235,710	35.1%^{4}F + 15.3% $5s^25p^2(^3P)6d\ ^4$P + 28.5% $5s^25p^2(^3P)6d\ ^4$D	0.369	0.427	0.337
	$^2P_{3/2}$	241,896	241,998	31.2%^{2}P + 33.3% $5s^25p^2(^3P)6d\ ^4$F + 22.7% $5s^25p^2(^3P)6d\ ^4$D	0.380	0.416	0.230
	$^4F_{7/2}$	242,080	242,086	63.1%^{4}F + 30.5% $5s^25p^2(^3P)6d\ ^4$D + 5.4% $5s^25p^2(^3P)6d\ ^2$F	0.744	0.796	0.679
	$^4D_{1/2}$	242,541	242,397	80.7%^{4}D + 12.6% $5s^25p^2(^3P)6d\ ^2$P + 5.5% $5s^25p^2(^3P)6d\ ^4$P	0.527	0.570	0.481
	$^4P_{5/2}$	242,534	242,571	28.3%^{4}P + 54.8% $5s^25p^2(^3P)6d\ ^4$F + 5.1% $5s^25p^2(^3P)6d\ ^4$D	0.338	0.389	0.302
	$^4D_{3/2}$	244,577	244,535	30.2%^{4}D + 35.1% $5s^25p^2(^3P)6d\ ^2$P + 14.7% $5s^25p^2(^3P)6d\ ^4$P	0.299	0.330	0.314
	$^2F_{5/2}$	244,722	244,609	65.4%^{2}F + 19.4% $5s^25p^2(^3P)6d\ ^4$P + 9.9% $5s^25p^2(^1D)6d\ ^2$F	0.277	0.326	0.223
	$^4D_{7/2}$	246,494	246,470	36.2%^{4}D + 26.4% $5s^25p^2(^3P)6d\ ^4$F + 18.9% $5s^25p^2(^1D)6d\ ^2$F	0.760	0.804	0.793
	$^4F_{9/2}$	246,662	246,625	80.2%^{4}F + 19.6% $5s^25p^2(^1D)6d\ ^2$G	0.845	0.891	0.818
	$^4D_{5/2}$	248,027	248,123	49.6%^{4}D + 24.6% $5s^25p^2(^3P)6d\ ^4$P + 16% $5s^25p^2(^1D)6d\ ^2$D	0.281	0.325	0.234
	$^4P_{3/2}$	248,565	248,623	57.2%^{4}P + 19.7% $5s^25p^2(^3P)6d\ ^4$D + 12.7% $5s^25p^2(^1D)6d\ ^2$P	0.259	0.313	0.205
	$^4P_{1/2}$	249,115	249,043	75.8%^{4}P + 11.7% $5s^25p^2(^1D)6d\ ^2$S + 4.9% $5s^25p^2(^1D)6d\ ^2$P	0.197	0.235	0.159
	$^2P_{1/2}$	250,691	250,595	69.6%^{2}P + 10.3% $5s^25p^2(^3P)6d\ ^4$D + 6.6% $5s^25p^2(^3P)7s\ ^2$P	0.213	0.244	0.165
	$^2F_{7/2}$	251,073	251,083	55.5%^{2}F + 22.9% $5s^25p^2(^1D)6d\ ^2$G + 17% $5s^25p^2(^3P)6d\ ^4$D	0.221	0.267	0.176
	$^2D_{5/2}$	251,211	251,204	61.9%^{2}D + 25% $5s^25p^2(^1D)6d\ ^2$F + 7.9% $5s^25p^2(^1D)6d\ ^2$D	0.203	0.251	0.144
	$^2D_{3/2}$	251,890	251,977	59.7%^{2}D + 14.1% $5s^25p^2(^1D)6d\ ^2$D + 8.3% $5s^25p^2(^1D)6d\ ^2$P	0.249	0.295	0.148
$5s^25p^2(^1D)6d$	$^2F_{7/2}$	260,362	260,428	58.7%^{2}F + 20.5% $5s^25p^2(^1D)6d\ ^2$G + 14.1% $5s^25p^2(^3P)6d\ ^4$D	0.546	0.614	0.527
	$^2G_{9/2}$	261,548	261,656	80.3%^{2}G + 19.6% $5s^25p^2(^3P)6d\ ^4$F	0.839	0.906	0.862
	$^2D_{5/2}$	262,379	262,321	44.1%^{2}D + 30.4% $5s^25p^2(^1D)6d\ ^2$F + 10% $5s^25p^2(^3P)6d\ ^4$D	0.196	0.230	0.155
	$^2D_{3/2}$	262,438	262,480	69.4%^{2}D + 7.5% $5s^25p^2(^1D)6d\ ^2$P + 6.9% $5s^25p^2(^3P)6d\ ^4$D	0.206	0.234	0.171
	$^2P_{1/2}$	262,937	262,904	85.4%^{2}P + 4.6% $5s^25p^2(^3P)6d\ ^2$P + 4.3% $5s^25p^2(^3P)6d\ ^4$D	0.323	0.395	0.286
	$^2G_{7/2}$	262,860	262,969	48.4%^{2}G + 22.2% $5s^25p^2(^3P)6d\ ^2$F + 19.3% $5s^25p^2(^1D)6d\ ^2$F	0.234	0.293	0.175

Table 1. *Cont.*

Designation		Energy (cm^{-1})		Composition	Lifetime(ns)		
		Exp.	Fitted		HFRa	HFR +CPa	MCDF Babushkin
$5s^25p^2(^1S)6d$	$^2F_{5/2}$	265,205	265,171	24.4%^{2}F + 22.1% $5s^25p^2(^3P)6d\ ^2D$ + 20.3% $5s^25p^2(^1D)6d\ ^2D$	0.216	0.253	0.157
	$^2P_{3/2}$	265,501	265,400	64.9%^{2}P + 9.7% $5s^25p^2(^3P)6d\ ^2P$ + 7.4% $5s^25p^2(^3P)6d\ ^2D$	0.278	0.334	0.346
	$^2S_{1/2}$	265,930	265,908	81.3%^{2}S + 11.4% $5s^25p^2(^3P)6d\ ^4P$ + 4.6% $5s^25p^2(^3P)6d\ ^2P$	0.198	0.226	0.171
	$^2D_{5/2}$	280,142	279,777	91.2%^{2}D + 2.8% $5s^25p^2(^3P)6d\ ^2F$ + 2.3% $5s^25p^2(^3P)6d\ ^4D$	0.361	0.421	0.316
	$^2D_{3/2}$	279,799	280,132	89.4%^{2}D + 4.3% $5s^25p^2(^3P)6d\ ^2D$ + 2.8% $5s^25p^2(^3P)6d\ ^4F$	0.244	0.293	0.211

In the analysis of spectroscopic data, we take into account isoelectronic trends, Ritz combinations, least-squares adjustment, and relative line intensities in order to identify 36 energy levels belonging to $5s^25p^2(6d+7s)$ configurations for the first time.

As for the isoelectronic sequence calculations used to produce the plots for observed minus calculated ("obs.-calc.") trends along the six first elements of the Sb sequence, we used the configurations $5s^25p^3$, $5s^25p^24f$, $5s^25p^26p$, $5s5p^36s$, $5s5p^37s$, $5s5p^35d$, $5s5p^3$ 6d, $5p^5$ for odd parity and $5s5p^4$, $5s^25p^25d$, $5s5p^35f$, $5s^25p^25g$, $5s^25p^26s$, $5s^25p^26d$, $5s^25p^27s$ for even parity. The calculations included core polarization effects (HFR+CP), with the values of α_d and rc taken from Table 2.

It must be noted that we implemented the modifications suggested by Kramida [25,26] to correct an error in Cowan's package in order to perform the calculations presented here.

Table 2. Values for polarizability α_d and cut-off radius r_c, used in antimony isoelectronic sequence calculations (HFR+CP). Here, a_0 is the Bohr radius.

Ion	α_d (a_0^3)	r_c (a_0)
Sb I	1.61620	1.33000
Te II	1.25140	1.27000
I III	0.99660	1.21000
Xe IV	0.81130	1.16000
Cs V	0.67210	1.11000
Ba VI	0.56500	1.07000

Data for isoelectronic analysis are from NIST [27] for Sb I, Te II, I III and from Sharman, Tauheed, and Rahimullah for Ba VI [28]. Our analysis is synthesized in Figures 1–3. Surely the LS coupling scheme is not the most appropriate to describe the 6d and 7s configurations, which we concluded after glancing over configuration purities; intermediate couplings provide better descriptions for these levels. We observed a strong eigenvector mixing for all elements studied. However, most of the isoelectronic data available for comparisons are described in the LS scheme, and that was the reason why we chose it.

There is no absolute scale for experimental intensity and therefore we only test its proportionality with the theoretical intensity. We do not include corrections due to the variation of plate reflectivity as a function of wavelength—there is no precise model for this. Our criterion for statistical correlation is to obtain a positive value as close as possible to the unit. Therefore, having a good statistical correlation supports our analysis, but it is just one of the analysis criteria.

The formula $I \propto \sigma gA$ from Cowan's book [17], page 403, tells us that line intensity is proportional to wavenumber σ and weighted transition probability. We analyzed the statistical correlation of the logarithm related to this quantity with the experimental line intensities, which is a visual estimate of the plate blackening (hence the logarithm), obtaining 0.20 for the array $6p - 6d$, 0.32 for $6p - 7s$, and 0.34 for $4f - 6d$. These values were acquired by the HFR+CPa calculation, which is close to HFRa and much better thanab initioHFR and HFR+CP calculations. We also performed a MCDF calculation for gA values. Its agreement with the experimental line intensity shows a poor correlation when compared with HFRa and HFR+CPa for $log(\sigma gA)$, that is, 0.06 for the $6p - 6d$ line array, 0.14 for $6p - 7s$, and 0.18 for $4f - 6d$. It is important to note that our MCDF calculations were performed using a non-current version of the GRASP code where more configurations could not be included. By using a newer version of Grasp codes it would be possible to expand the number of configurations to get better results, which could be more competitive to HFRa and HFR + CPa methods

To understand thesignificance of these values, we compared our values of gA with the experimental values that are in the paper by Bertuccelli et al. [16]. Similarly to them, only 25% of our gA values (HFR+CPa) are within the experimental error. However, a statistical correlation of 0.94 indicates that our values are very linearly proportional to their experiment. When considering the same lines of [16], but substituting their experimental gA values by our estimates for line intensity, correlation

with HFR+CPa $log(\sigma gA)$ results in 0.33 for the $6s-6p$ line array, 0.48 for $5d-6p$, and 0.50 for $5d-4f$. Therefore, we can conclude that the calculated σ gA values support our line classification with reasonable agreement.

It is important to note that in this spectral analysis all new levels but two are classified on the basis of two or more lines. The level $^4F_{5/2}$ is a classification attempt based on the only possible line in our spectrograms at 1801.53 Å, a transition with 4f:$^4G_{5/2}$, the strongest spontaneous emission from this level. However, this value does not fit the isoelectronic "obs.-calc." curve. We remove this problem by switching the positions of levels 6d:$^4P_{5/2}$ and 6d:$^4F_{5/2}$ for Xe IV in the isoelectronic analysis. An intense mixing for 6d:$^4P_{5/2}$, $^4D_{5/2}$, and $^4F_{5/2}$ makes the components for the eigenvectors exchange their intensity along with the four first elements, and our choice grouped the energy of the respective multiplets.

Due to similar reasons, we also switched $^4D_{5/2}$ and $^4P_{5/2}$ energy levels for Te III and I III in the respective isoelectronic sequences.

The other level that only has one observed transition is (^{1}S)6d: $^2D_{3/2}$ that we confirm by our isoelectronic analysis and considering the good agreement in the least squares fit calculation.

There is not much data available for isoelectronic analysis. The lack of information on Cesium and the composition mixing makes level designation a challenge. However, the isoelectronic sequences agree reasonably well with our designations.

Table 3 shows 163 Xe IV lines classified for the first time for transitions involving $5s^25p^2$(6d+7s) energy levels. We also calculated the weighted transition probability rate gA, where g is the statistical weight 2J+1 of the upper level. We presented gA values obtained from the four methods studied: With and without optimized parameters obtained from least-squares calculations, and with and without core polarization effects for wavefunctions and reduced matrix elements calculations.In these methods, we used the same configuration sets as in [15], that is, $5s^25p^3$, 5^25p^2 (4f+6p), 5s $5p^35d$, $5p^5$ and $5s5p^4$, $5s^25p^2$ (6s+7s+5d+6d) configurations for odd and even parities, respectively.

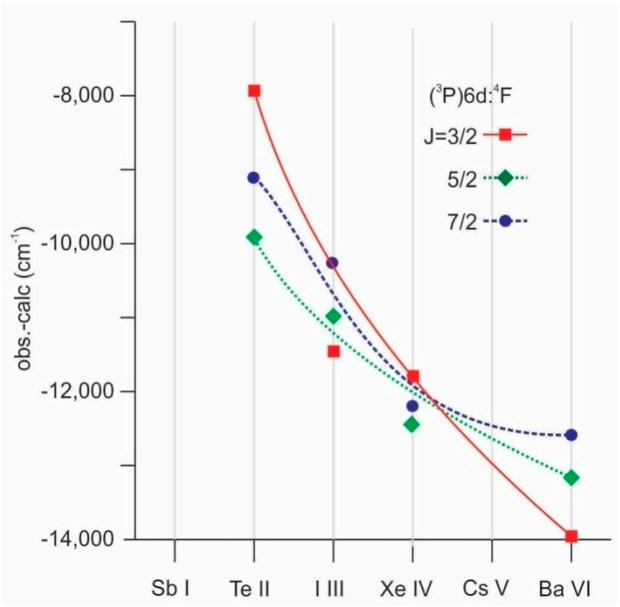

Figure 1. Isoelectronic trend for the multiplet (^{3}P) ^{4}F energy levels of the $5s^25p^2$ 6d configuration.

Table 3. Transitions and weighted transition rates for Xe IV.

Int	λ (Å)	Energy (cm^{-1})		Designation		Weighted Transition Rates—gA (s^{-1})		
		Lower	Upper	Lower	Upper	Adjusted		
		Level	Level	Level	Level	HFRa	HFR+CPa	HFR+CP
1	1078.51	190,793	283,512	$5s^25p^2(^3P)6p\ ^4D_{3/2}$	$5s^25p^2(^1S)7s\ ^2S_{1/2}$	6.623×10^6	3.771×10^6	9.474×10^4
3	1115.44	193,861	283,512	$5s^25p^2(^3P)6p\ ^2S_{1/2}$	$5s^25p^2(^1S)7s\ ^2S_{1/2}$	8.542×10^4	8.067×10^4	2.572×10^5
2	1139.89	195,785	283,512	$5s^25p^2(^3P)4f\ ^4D_{3/2}$	$5s^25p^2(^1S)7s\ ^2S_{1/2}$	2.395×10^4	2.750×10^3	2.061×10^5
2	1151.31	196,655	283,512	$5s^25p^2(^3P)4f\ ^4D_{1/2}$	$5s^25p^2(^1S)7s\ ^2S_{1/2}$	9.396×10^3	6.026×10^3	4.447×10^4
2	1212.39	201,028	283,512	$5s^25p^2(^3P)6p\ ^4S_{3/2}$	$5s^25p^2(^1S)7s\ ^2S_{1/2}$	1.932×10^4	5.698×10^4	7.434×10^6
2	1240.09	182,219	262,860	$5s^25p^2(^3P)4f\ ^4G_{7/2}$	$5s^25p^2(^1D)6d\ ^2G_{7/2}$	1.210×10^6	9.729×10^5	9.768×10^5
2	1259.87	204,140	283,512	$5s^25p^2(^3P)6p\ ^4P_{3/2}$	$5s^25p^2(^1S)7s\ ^2S_{1/2}$	7.200×10^6	6.818×10^6	2.361×10^5
1	1291.10	206,061	283,512	$5s^25p^2(^3P)6p\ ^2P_{3/2}$	$5s^25p^2(^1S)7s\ ^2S_{1/2}$	1.288×10^7	1.543×10^7	1.891×10^7
2	1326.93	189,842	265,205	$5s^25p^2(^3P)4f\ ^4D_{7/2}$	$5s^25p^2(^1D)6d\ ^2F_{5/2}$	3.168×10^7	2.181×10^7	2.609×10^7
2	1340.56	205,205	279,799	$5s^25p^2(^1D)4f\ ^2F_{5/2}$	$5s^25p^2(^1S)6d^2D_{3/2}$	7.092×10^6	1.296×10^6	1.155×10^7
1	1357.65	188,721	262,379	$5s^25p^2(^3P)4f\ ^2D_{5/2}$	$5s^25p^2(^1D)6d\ ^2D_{5/2}$	4.998×10^6	4.123×10^6	3.280×10^6
2	1386.74	188,252	260,362	$5s^25p^2(^3P)4f\ ^4G_{9/2}$	$5s^25p^2(^1D)6d\ ^2F_{7/2}$	1.755×10^6	1.789×10^6	1.046×10^6
1	1394.58	189,842	261,548	$5s^25p^2(^3P)4f\ ^4D_{7/2}$	$5s^25p^2(^1D)6d\ ^2G_{9/2}$	3.174×10^3	7.428×10^3	7.100×10^3
1	1419.25	191,978	262,438	$5s^25p^2(^3P)4f\ ^4D_{5/2}$	$5s^25p^2(^1D)6d\ ^2D_{3/2}$	5.438×10^5	2.925×10^5	2.289×10^5
1	1420.42	191,978	262,379	$5s^25p^2(^3P)4f\ ^4D_{5/2}$	$5s^25p^2(^1D)6d\ ^2D_{5/2}$	4.326×10^6	3.840×10^6	7.217×10^6
1	1430.66	196,725	266,623	$5s^25p^2(^3P)6p\ ^2D_{3/2}$	$5s^25p^2(^1D)7s\ ^2D_{3/2}$	1.565×10^7	9.181×10^6	3.609×10^7
1	1434.39	195,785	265,501	$5s^25p^2(^3P)4f\ ^4D_{3/2}$	$5s^25p^2(^1D)6d\ ^2P_{3/2}$	5.789×10^6	3.652×10^6	2.398×10^5
1	1477.52	198,943	266,623	$5s^25p^2(^3P)6p\ ^4D_{5/2}$	$5s^25p^2(^1D)7s\ ^2D_{3/2}$	1.049×10^6	2.225×10^5	3.155×10^6
1	1496.21	186,109	252,943	$5s^25p^2(^3P)6p\ ^4D_{1/2}$	$5s^25p^2(^3P)7s\ ^2P_{3/2}$	2.673×10^7	3.318×10^7	1.700×10^7
2	1507.08	196,506	262,860	$5s^25p^2(^3P)4f\ ^4F_{5/2}$	$5s^25p^2(^1D)6d\ ^2G_{7/2}$	1.549×10^4	5.596×10^5	9.001×10^6
1	1521.44	200,899	266,623	$5s^25p^2(^3P)6p\ ^4P_{1/2}$	$5s^25p^2(^1D)7s\ ^2D_{3/2}$	2.177×10^5	1.502×10^4	1.926×10^5
9	1551.78	182,219	246,662	$5s^25p^2(^3P)4f\ ^4G_{7/2}$	$5s^25p^2(^3P)6d^4F_{9/2}$	1.587×10^7	1.008×10^7	9.882×10^6
4	1552.22	180,152	244,577	$5s^25p^2(^3P)4f\ ^4G_{5/2}$	$5s^25p^2(^3P)6d^4D_{3/2}$	8.606×10^5	2.951×10^5	2.936×10^7
7	1573.83	187,533	251,073	$5s^25p^2(^3P)4f\ ^2G_{7/2}$	$5s^25p^2(^3P)6d^2F_{7/2}$	1.203×10^7	7.570×10^6	4.904×10^6
7	1615.28	201,028	262,937	$5s^25p^2(^3P)6p\ ^4S_{3/2}$	$5s^25p^2(^1D)6d\ ^2P_{1/2}$	6.055×10^7	4.595×10^7	5.730×10^6
6	1618.41	204,140	265,930	$5s^25p^2(^3P)6p\ ^4P_{3/2}$	$5s^25p^2(^1D)6d\ ^2S_{1/2}$	1.484×10^7	2.801×10^6	8.778×10^5
1	1626.69	186,109	247,583	$5s^25p^2(^3P)6p\ ^4D_{1/2}$	$5s^25p^2(^3P)7s\ ^2P_{1/2}$	2.319×10^7	2.526×10^7	2.055×10^7
3	1645.20	202,076	262,860	$5s^25p^2(^3P)4f\ ^4F_{9/2}$	$5s^25p^2(^1D)6d\ ^2G_{7/2}$	6.376×10^7	4.843×10^7	1.556×10^8
5	1650.75	186,109	246,689	$5s^25p^2(^3P)6p\ ^4D_{1/2}$	$5s^25p^2(^3P)7s\ ^4P_{3/2}$	1.606×10^6	1.586×10^6	2.029×10^6
7	1658.00	182,219	242,534	$5s^25p^2(^3P)4f\ ^4G_{7/2}$	$5s^25p^2(^3P)6d^4F_{5/2}$	3.389×10^7	2.586×10^7	3.940×10^8
2	1665.77	191,858	251,890	$5s^25p^2(^3P)4f\ ^4F_{3/2}$	$5s^25p^2(^3P)6d^2D_{3/2}$	2.043×10^7	2.421×10^7	7.476×10^5

Table 3. *Cont.*

Int	λ (Å)	Energy (cm^{-1})		Designation		Weighted Transition Rates—gA (s^{-1})		
		Lower	Upper	Lower	Upper	Adjusted		
		Level	Level	Level	Level	HFRa	HFR+CPa	HFR+CP
4	1666.86	191,858	251,851	$5s^25p^2(^3P)4f\ ^4F_{3/2}$	$5s^25p^2(^3P)7s\ ^4P_{5/2}$	1.451×10^6	7.145×10^4	1.065×10^5
5	1670.08	200,486	260,362	$5s^25p^2(^3P)6p\ ^2D_{5/2}$	$5s^25p^2(^1D)6d\ ^2F_{7/2}$	1.713×10^7	1.995×10^7	7.747×10^7
6	1670.33	206,061	265,930	$5s^25p^2(^3P)6p\ ^2P_{3/2}$	$5s^25p^2(^1D)6d\ ^2S_{1/2}$	1.361×10^8	1.050×10^8	1.881×10^8
3	1670.60	182,219	242,080	$5s^25p^2(^3P)4f\ ^4G_{7/2}$	$5s^25p^2(^3P)6d^4F_{7/2}$	1.019×10^7	7.394×10^6	1.384×10^7
3	1678.74	207,057	266,623	$5s^25p^2(^3P)6p\ ^4P_{5/2}$	$5s^25p^2(^1D)7s\ ^2D_{3/2}$	1.362×10^8	8.177×10^7	6.031×10^6
5	1681.48	202,076	261,548	$5s^25p^2(^3P)4f\ ^4F_{9/2}$	$5s^25p^2(^1D)6d\ ^2G_{9/2}$	5.905×10^7	4.145×10^7	2.013×10^7
7	1686.18	188,721	248,027	$5s^25p^2(^3P)4f\ ^2D_{5/2}$	$5s^25p^2(^3P)6d^4D_{5/2}$	3.718×10^6	2.399×10^6	3.658×10^6
4	1691.19	187,533	246,662	$5s^25p^2(^3P)4f\ ^2G_{7/2}$	$5s^25p^2(^3P)6d^4F_{9/2}$	1.109×10^7	8.797×10^6	2.209×10^7
4	1692.52	193,861	252,943	$5s^25p^2(^3P)6p\ ^2S_{1/2}$	$5s^25p^2(^3P)7s\ ^2P_{3/2}$	6.667×10^7	7.498×10^7	2.117×10^7
6	1694.50	224,498	283,512	$5s^25p^2(^1D)6p\ ^2P_{3/2}$	$5s^25p^2(^1S)7s\ ^2S_{1/2}$	3.004×10^6	1.175×10^7	3.405×10^5
7	1709.63	206,713	265,205	$5s^25p^2(^1D)4f\ ^2G_{7/2}$	$5s^25p^2(^1D)6d\ ^2F_{5/2}$	1.281×10^7	1.748×10^6	2.737×10^7
6	1710.31	186,109	244,577	$5s^25p^2(^3P)6p\ ^4D_{1/2}$	$5s^25p^2(^3P)6d^4D_{3/2}$	9.124×10^7	1.199×10^8	1.594×10^8
2	1712.04	188,252	246,662	$5s^25p^2(^3P)4f\ ^4G_{9/2}$	$5s^25p^2(^3P)6d^4F_{9/2}$	3.385×10^7	2.261×10^7	2.546×10^7
4	1730.94	188,721	246,494	$5s^25p^2(^3P)4f\ ^2D_{5/2}$	$5s^25p^2(^3P)6d^4D_{7/2}$	1.525×10^6	8.100×10^4	1.367×10^6
4	1730.94	190,793	248,565	$5s^25p^2(^3P)6p\ ^4D_{3/2}$	$5s^25p^2(^3P)6d^4P_{3/2}$	2.244×10^6	7.523×10^6	2.589×10^6
6	1734.81	205,217	262,860	$5s^25p^2(^1D)4f\ ^2F_{7/2}$	$5s^25p^2(^1D)6d\ ^2G_{7/2}$	3.324×10^7	2.371×10^7	6.740×10^7
5	1747.19	190,793	248,027	$5s^25p^2(^3P)6p\ ^4D_{3/2}$	$5s^25p^2(^3P)6d^4D_{5/2}$	5.268×10^6	7.486×10^6	2.265×10^4
4	1749.08	205,205	262,379	$5s^25p^2(^1D)4f\ ^2F_{5/2}$	$5s^25p^2(^1D)6d\ ^2D_{5/2}$	8.193×10^7	4.709×10^7	4.908×10^8
4	1749.39	205,217	262.,379	$5s^25p^2(^1D)4f\ ^2F_{7/2}$	$5s^25p^2(^1D)6d\ ^2D_{5/2}$	1.931×10^8	9.089×10^7	1.992×10^8
4	1759.59	193,861	250,691	$5s^25p^2(^3P)6p\ ^2S_{1/2}$	$5s^25p^2(^3P)6d^2P_{1/2}$	1.497×10^8	1.798×10^8	1.994×10^8
4	1765.15	189,842	246,494	$5s^25p^2(^3P)4f\ ^4D_{7/2}$	$5s^25p^2(^3P)6d^4D_{7/2}$	1.249×10^7	9.511×10^6	2.037×10^7
6	1765.42	206,216	262,860	$5s^25p^2(^1D)4f\ ^2H_{9/2}$	$5s^25p^2(^1D)6d\ ^2G_{7/2}$	1.762×10^7	1.752×10^7	5.048×10^5
3	1778.77	196,725	252,943	$5s^25p^2(^3P)6p\ ^2D_{3/2}$	$5s^25p^2(^3P)7s\ ^2P_{3/2}$	9.427×10^7	8.509×10^7	4.613×10^8
4	1780.72	209,344	265,501	$5s^25p^2(^3P)6p\ ^2P_{1/2}$	$5s^25p^2(^1D)6d\ ^2P_{3/2}$	1.806×10^8	2.079×10^8	4.567×10^8
4	1781.04	206,713	262,860	$5s^25p^2(^1D)4f\ ^2G_{7/2}$	$5s^25p^2(^1D)6d\ ^2G_{7/2}$	1.404×10^7	1.256×10^7	5.619×10^6
4	1782.39	195,785	251,890	$5s^25p^2(^3P)4f\ ^4D_{3/2}$	$5s^25p^2(^3P)6d^2D_{3/2}$	1.465×10^8	1.280×10^8	3.935×10^7
3	1784.18	191,978	248,027	$5s^25p^2(^3P)4f\ ^4D_{5/2}$	$5s^25p^2(^3P)6d^4D_{5/2}$	1.175×10^7	6.655×10^6	1.529×10^7
4	1789.02	190,793	246,689	$5s^25p^2(^3P)6p\ ^4D_{3/2}$	$5s^25p^2(^3P)7s\ ^4P_{3/2}$	1.186×10^8	9.404×10^7	1.597×10^8
4	1797.14	224,498	280,142	$5s^25p^2(^1D)6p\ ^2P_{3/2}$	$5s^25p^2(^1S)6d^2D_{5/2}$	5.493×10^7	1.126×10^8	1.487×10^7
4	1800.99	196,325	251,851	$5s^25p^2(^3P)4f\ ^4F_{7/2}$	$5s^25p^2(^3P)7s\ ^4P_{5/2}$	2.801×10^6	7.025×10^5	3.792×10^5
7	1801.53	180,152	235,660	$5s^25p^2(^3P)4f\ ^4G_{5/2}$	$5s^25p^2(^3P)6d^4P_{5/2}$	2.977×10^7	2.086×10^7	8.452×10^6

Table 3. *Cont.*

Int	λ (Å)	Energy (cm^{-1})		Designation		Weighted Transition Rates—gA (s^{-1})		
		Lower	Upper	Lower	Upper	Adjusted		
		Level	Level	Level	Level	HFRa	HFR+CPa	HFR+CP
6	1807.29	206,216	261,548	$5s^25p^2(^1D)4f\ ^2H_{9/2}$	$5s^25p^2(^1D)6d\ ^2G_{9/2}$	3.229×10^7	2.550×10^7	2.172×10^7
6	1813.02	205,205	260,362	$5s^25p^2(^1D)4f\ ^2F_{5/2}$	$5s^25p^2(^1D)6d\ ^2F_{7/2}$	2.235×10^7	3.081×10^7	2.006×10^7
3	1813.39	205,217	260,362	$5s^25p^2(^1D)4f\ ^2F_{7/2}$	$5s^25p^2(^1D)6d\ ^2F_{7/2}$	1.362×10^8	1.150×10^8	1.140×10^8
4	1813.95	196,725	251,851	$5s^25p^2(^3P)6p\ ^2D_{3/2}$	$5s^25p^2(^3P)7s\ ^4P_{5/2}$	1.231×10^8	9.434×10^7	3.600×10^4
1	1821.29	195,785	250,691	$5s^25p^2(^3P)4f\ ^4D_{3/2}$	$5s^25p^2(^3P)6d^2P_{1/2}$	2.749×10^7	2.287×10^7	5.120×10^6
8	1822.13	189,842	244,722	$5s^25p^2(^3P)4f\ ^4D_{7/2}$	$5s^25p^2(^3P)6d^2F_{5/2}$	4.321×10^8	3.081×10^8	3.510×10^8
3	1823.68	206,713	261,548	$5s^25p^2(^1D)4f\ ^2G_{7/2}$	$5s^25p^2(^1D)6d\ ^2G_{9/2}$	1.275×10^8	1.092×10^8	3.008×10^8
5	1833.29	187,533	242,080	$5s^25p^2(^3P)4f\ ^2G_{7/2}$	$5s^25p^2(^3P)6d^4F_{7/2}$	5.893×10^7	4.396×10^7	5.539×10^7
3	1853.01	196,725	250,691	$5s^25p^2(^3P)6p\ ^2D_{3/2}$	$5s^25p^2(^3P)6d^2P_{1/2}$	2.641×10^6	8.155×10^5	6.555×10^7
5	1854.27	190,793	244,722	$5s^25p^2(^3P)6p\ ^4D_{3/2}$	$5s^25p^2(^3P)6d^2F_{5/2}$	5.464×10^5	1.286×10^6	3.530×10^6
4	1858.13	208,621	262,438	$5s^25p^2(^3P)4f\ ^2F_{5/2}$	$5s^25p^2(^1D)6d\ ^2D_{3/2}$	1.071×10^8	9.091×10^7	2.376×10^7
3	1863.98	206,713	260,362	$5s^25p^2(^1D)4f\ ^2G_{7/2}$	$5s^25p^2(^1D)6d\ ^2F_{7/2}$	1.796×10^4	1.370×10^6	2.856×10^7
2	1874.10	188,721	242,080	$5s^25p^2(^3P)4f\ ^2D_{5/2}$	$5s^25p^2(^3P)6d^4F_{7/2}$	7.040×10^6	7.698×10^6	1.683×10^7
5	1883.46	209,344	262,438	$5s^25p^2(^3P)6p\ ^2P_{1/2}$	$5s^25p^2(^1D)6d\ ^2D_{3/2}$	4.162×10^7	3.800×10^7	7.917×10^7
6	1890.04	198,943	251,851	$5s^25p^2(^3P)6p\ ^4D_{5/2}$	$5s^25p^2(^3P)7s\ ^4P_{5/2}$	4.565×10^8	3.836×10^8	2.559×10^6
3	1894.62	195,785	248,565	$5s^25p^2(^3P)4f\ ^4D_{3/2}$	$5s^25p^2(^3P)6d^4P_{3/2}$	9.841×10^6	6.703×10^6	2.840×10^8
7	1897.88	189,842	242,534	$5s^25p^2(^3P)4f\ ^4D_{7/2}$	$5s^25p^2(^3P)6d^4F_{5/2}$	4.812×10^7	2.681×10^7	1.772×10^6
5	1901.17	191,978	244,577	$5s^25p^2(^3P)4f\ ^4D_{5/2}$	$5s^25p^2(^3P)6d^4D_{3/2}$	2.501×10^8	1.785×10^8	1.428×10^4
4	1905.07	199,397	251,890	$5s^25p^2(^3P)4f\ ^2D_{3/2}$	$5s^25p^2(^3P)6d^2D_{3/2}$	5.527×10^7	5.888×10^7	2.821×10^7
7	1906.20	196,655	249,115	$5s^25p^2(^3P)4f\ ^4D_{1/2}$	$5s^25p^2(^3P)6d^4P_{1/2}$	9.874×10^7	7.103×10^7	6.996×10^7
6	1913.18	198,943	251,211	$5s^25p^2(^3P)6p\ ^4D_{5/2}$	$5s^25p^2(^3P)6d^2D_{5/2}$	2.215×10^8	1.343×10^8	8.697×10^6
8	1914.28	189,842	242,080	$5s^25p^2(^3P)4f\ ^4D_{7/2}$	$5s^25p^2(^3P)6d^4F_{7/2}$	3.153×10^7	2.053×10^7	1.020×10^7
4	1918.27	198,943	251,073	$5s^25p^2(^3P)6p\ ^4D_{5/2}$	$5s^25p^2(^3P)6d^2F_{7/2}$	3.502×10^8	2.137×10^8	1.380×10^7
5	1929.04	196,725	248,565	$5s^25p^2(^3P)6p\ ^2D_{3/2}$	$5s^25p^2(^3P)6d^4P_{3/2}$	3.905×10^8	2.829×10^8	8.032×10^6
2	1930.57	195,785	247,583	$5s^25p^2(^3P)4f\ ^4D_{3/2}$	$5s^25p^2(^3P)7s\ ^2P_{1/2}$	1.205×10^8	1.336×10^8	5.103×10^8
4	1960.89	215,626	266,623	$5s^25p^2(^1D)6p\ ^2F_{5/2}$	$5s^25p^2(^1D)7s\ ^2D_{3/2}$	1.521×10^9	1.359×10^9	9.246×10^8
6	1961.19	200,899	251,890	$5s^25p^2(^3P)6p\ ^4P_{1/2}$	$5s^25p^2(^3P)6d^2D_{3/2}$	1.312×10^7	1.068×10^7	3.950×10^7
4	1966.19	196,725	247,583	$5s^25p^2(^3P)6p\ ^2D_{3/2}$	$5s^25p^2(^3P)7s\ ^2P_{1/2}$	5.960×10^8	5.444×10^8	4.223×10^8
2	1967.55	201,028	251,851	$5s^25p^2(^3P)6p\ ^4S_{3/2}$	$5s^25p^2(^3P)7s\ ^4P_{5/2}$	7.882×10^7	1.314×10^8	1.316×10^9
7	1972.35	232,811	283,512	$5s^25p^2(^1S)6p\ ^2P_{1/2}$	$5s^25p^2(^1S)7s\ ^2S_{1/2}$	8.420×10^8	7.097×10^8	7.885×10^8
2	1973.04	191,858	242,541	$5s^25p^2(^3P)4f\ ^4F_{3/2}$	$5s^25p^2(^3P)6d^4D_{1/2}$	1.839×10^8	1.453×10^8	1.563×10^8

Table 3. *Cont.*

Int	λ (Å)	Energy (cm^{-1})		Designation		Weighted Transition Rates—gA (s^{-1})		
		Lower	Upper	Lower	Upper	Adjusted		
		Level	Level	Level	Level	HFRa	HFR+CPa	HFR+CP
2	1976.77	200,486	251,073	$5s^25p^2(^3P)6p\ ^2D_{5/2}$	$5s^25p^2(^3P)6d^2F_{7/2}$	1.277×10^9	1.374×10^9	2.637×10^8
5	1980.87	216,141	266,623	$5s^25p^2(^1D)6p\ ^2D_{3/2}$	$5s^25p^2(^1D)7s\ ^2D_{3/2}$	2.008×10^8	2.357×10^8	8.700×10^7
5	2007.72	200,899	250,691	$5s^25p^2(^3P)6p\ ^4P_{1/2}$	$5s^25p^2(^3P)6d^2P_{1/2}$	1.785×10^8	1.802×10^8	2.370×10^8
2	2010.79	199,397	249,115	$5s^25p^2(^3P)4f\ ^2D_{3/2}$	$5s^25p^2(^3P)6d^4P_{1/2}$	1.249×10^7	4.943×10^6	4.035×10^7
8	2014.59	198,943	248,565	$5s^25p^2(^3P)6p\ ^4D_{5/2}$	$5s^25p^2(^3P)6d^4P_{3/2}$	3.953×10^7	1.658×10^7	7.665×10^7
1	2016.33	215,626	265,205	$5s^25p^2(^1D)6p\ ^2F_{5/2}$	$5s^25p^2(^1D)6d\ ^2F_{5/2}$	8.577×10^8	4.038×10^8	6.030×10^8
3	2022.77	216,911	266,331	$5s^25p^2(^1D)6p\ ^2D_{5/2}$	$5s^25p^2(^1D)7s\ ^2D_{5/2}$	5.091×10^8	3.580×10^8	5.529×10^8
4	2025.24	216,141	265,501	$5s^25p^2(^1D)6p\ ^2D_{3/2}$	$5s^25p^2(^1D)6d\ ^2P_{3/2}$	9.701×10^7	4.608×10^7	3.323×10^7
2	2033.21	199,397	248,565	$5s^25p^2(^3P)4f\ ^2D_{3/2}$	$5s^25p^2(^3P)6d^4P_{3/2}$	2.115×10^5	1.036×10^6	2.923×10^7
1	2036.36	217,240	266,331	$5s^25p^2(^1D)6p\ ^2F_{7/2}$	$5s^25p^2(^1D)7s\ ^2D_{5/2}$	2.256×10^9	1.670×10^9	1.307×10^9
1	2036.71	198,943	248,027	$5s^25p^2(^3P)6p\ ^4D_{5/2}$	$5s^25p^2(^3P)6d^4D_{5/2}$	6.800×10^8	5.262×10^8	4.763×10^7
1	2048.41	204,140	252,943	$5s^25p^2(^3P)6p\ ^4P_{3/2}$	$5s^25p^2(^3P)7s\ ^2P_{3/2}$	1.331×10^6	2.474×10^6	4.866×10^7
2	2071.42	202,951	251,211	$5s^25p^2(^3P)6p\ ^4D_{7/2}$	$5s^25p^2(^3P)6d^2D_{5/2}$	3.115×10^7	2.743×10^7	1.306×10^8
5	2071.80	196,325	244,577	$5s^25p^2(^3P)4f\ ^4F_{7/2}$	$5s^25p^2(^3P)6d^4D_{3/2}$	1.306×10^8	1.306×10^8	1.306×10^8
7	2073.30	196,506	244,722	$5s^25p^2(^3P)4f\ ^4F_{5/2}$	$5s^25p^2(^3P)6d^2F_{5/2}$	2.372×10^7	1.778×10^7	7.477×10^7
7	2073.30	200,899	249,115	$5s^25p^2(^3P)6p\ ^4P_{1/2}$	$5s^25p^2(^3P)6d^4P_{1/2}$	8.505×10^7	7.698×10^7	7.506×10^7
3	2074.74	186,109	234,291	$5s^25p^2(^3P)6p\ ^4D_{1/2}$	$5s^25p^2(^3P)6d^4F_{3/2}$	4.587×10^9	4.423×10^9	4.385×10^9
3	2077.37	202,951	251,073	$5s^25p^2(^3P)6p\ ^4D_{7/2}$	$5s^25p^2(^3P)6d^2F_{7/2}$	3.747×10^8	3.835×10^8	5.358×10^8
3	2078.87	201,028	249,115	$5s^25p^2(^3P)6p\ ^4S_{3/2}$	$5s^25p^2(^3P)6d^4P_{1/2}$	8.110×10^7	1.455×10^8	2.137×10^9
9	2079.23	200,486	248,565	$5s^25p^2(^3P)6p\ ^2D_{5/2}$	$5s^25p^2(^3P)6d^4P_{3/2}$	1.066×10^9	1.029×10^9	1.502×10^7
3	2081.10	193,861	241,896	$5s^25p^2(^3P)6p\ ^2S_{1/2}$	$5s^25p^2(^3P)6d^2P_{3/2}$	2.500×10^9	2.376×10^9	9.586×10^8
2	2093.75	198,943	246,689	$5s^25p^2(^3P)6p\ ^4D_{5/2}$	$5s^25p^2(^3P)7s\ ^4P_{3/2}$	1.854×10^9	1.981×10^9	2.738×10^8
2	2094.11	205,205	252,943	$5s^25p^2(^1D)4f\ ^2F_{5/2}$	$5s^25p^2(^3P)7s\ ^2P_{3/2}$	3.332×10^7	3.297×10^7	3.947×10^8
6	2102.94	201,028	248,565	$5s^25p^2(^3P)6p\ ^4S_{3/2}$	$5s^25p^2(^3P)6d^4P_{3/2}$	9.059×10^7	1.802×10^8	2.927×10^9
2	2136.22	216,141	262,937	$5s^25p^2(^1D)6p\ ^2D_{3/2}$	$5s^25p^2(^1D)6d\ ^2P_{1/2}$	8.568×10^8	8.495×10^8	6.086×10^8
2	2147.31	201,028	247,583	$5s^25p^2(^3P)6p\ ^4S_{3/2}$	$5s^25p^2(^3P)7s\ ^2P_{1/2}$	5.096×10^8	5.571×10^8	5.606×10^5
4	2149.87	219,002	265,501	$5s^25p^2(^1D)4f\ ^2D_{5/2}$	$5s^25p^2(^1D)6d\ ^2P_{3/2}$	1.852×10^8	1.390×10^8	3.914×10^7
2	2183.24	206,061	251,851	$5s^25p^2(^3P)6p\ ^2P_{3/2}$	$5s^25p^2(^3P)7s\ ^4P_{5/2}$	2.778×10^7	7.787×10^6	1.668×10^8
2	2183.24	200,899	246,689	$5s^25p^2(^3P)6p\ ^4P_{1/2}$	$5s^25p^2(^3P)7s\ ^4P_{3/2}$	6.598×10^8	6.667×10^8	1.009×10^9
3	2207.67	193,861	239,145	$5s^25p^2(^3P)6p\ ^2S_{1/2}$	$5s^25p^2(^3P)7s\ ^4P_{1/2}$	4.086×10^6	6.405×10^6	7.185×10^6
1	2214.68	217,240	262,379	$5s^25p^2(^1D)6p\ ^2F_{7/2}$	$5s^25p^2(^1D)6d\ ^2D_{5/2}$	1.526×10^8	9.614×10^7	2.354×10^8

Table 3. *Cont.*

Int	λ (Å)	Energy (cm^{-1})		Designation		Weighted Transition Rates—gA (s^{-1})		
		Lower	Upper	Lower	Upper	Adjusted		
		Level	Level	Level	Level	HFRa	HFR+CPa	HFR+CP
1	2239.94	206,061	250,691	$5s^25p^2(^3P)6p\ ^2P_{3/2}$	$5s^25p^2(^3P)6d^2P_{1/2}$	2.758×10^8	2.702×10^8	3.217×10^8
1	2242.39	235,561	280,142	$5s^25p^2(^1S)6p\ ^2P_{3/2}$	$5s^25p^2(^1S)6d^2D_{5/2}$	6.465×10^9	6.274×10	6.193×10^9
5	2295.89	202,951	246,494	$5s^25p^2(^3P)6p\ ^4D_{7/2}$	$5s^25p^2(^3P)6d^4D_{7/2}$	2.371×10^9	2.357×10^9	2.815×10^9
1	2298.23	190,793	234,291	$5s^25p^2(^3P)6p\ ^4D_{3/2}$	$5s^25p^2(^3P)6d^4F_{3/2}$	4.862×10^8	4.099×10^8	5.482×10^8
1	2317.55	199,397	242,534	$5s^25p^2(^3P)4f\ ^2D_{3/2}$	$5s^25p^2(^3P)6d^4F_{5/2}$	3.469×10^8	4.846×10^8	1.949×10^5
3	2407.63	206,061	247,583	$5s^25p^2(^3P)6p\ ^2P_{3/2}$	$5s^25p^2(^3P)7s\ ^2P_{1/2}$	1.076×10^8	9.367×10^7	7.285×10^7
6	2408.41	207,057	248,565	$5s^25p^2(^3P)6p\ ^4P_{5/2}$	$5s^25p^2(^3P)6d^4P_{3/2}$	2.324×10^8	2.041×10^8	1.291×10^9
2	2472.25	204,140	244,577	$5s^25p^2(^3P)6p\ ^4P_{3/2}$	$5s^25p^2(^3P)6d^4D_{3/2}$	2.832×10^7	5.368×10^7	1.035×10^8
3	2498.99	202,076	242,080	$5s^25p^2(^3P)4f\ ^4F_{9/2}$	$5s^25p^2(^3P)6d^4F_{7/2}$	6.998×10^6	4.645×10^6	9.367×10^5
3	2502.73	208,621	248,565	$5s^25p^2(^3P)4f\ ^2F_{5/2}$	$5s^25p^2(^3P)6d^4P_{3/2}$	4.929×10^7	7.502×10^7	5.397×10^5
1	2595.56	206,061	244,577	$5s^25p^2(^3P)6p\ ^2P_{3/2}$	$5s^25p^2(^3P)6d^4D_{3/2}$	4.640×10^8	4.162×10^8	4.734×10^7
1	2596.23	195,785	234,291	$5s^25p^2(^3P)4f\ ^4D_{3/2}$	$5s^25p^2(^3P)6d^4F_{3/2}$	6.854×10^6	4.678×10^6	1.515×10^6
1	2603.52	204,140	242,541	$5s^25p^2(^3P)6p\ ^4P_{3/2}$	$5s^25p^2(^3P)6d^4D_{1/2}$	1.003×10^7	1.586×10^7	4.086×10^7
2	2622.74	201,028	239,.145	$5s^25p^2(^3P)6p\ ^4S_{3/2}$	$5s^25p^2(^3P)7s\ ^4P_{1/2}$	1.124×10^7	6.599×10^6	5.223×10^6
1	2789.76	206,.061	241,896	$5s^25p^2(^3P)6p\ ^2P_{3/2}$	$5s^25p^2(^3P)6d^2P_{3/2}$	4.024×10^7	3.675×10^7	3.847×10^8
1	2855.73	204,140	239,145	$5s^25p^2(^3P)6p\ ^4P_{3/2}$	$5s^25p^2(^3P)7s\ ^4P_{1/2}$	3.366×10^6	1.750×10^6	2.920×10^7
4	3021.77	206,061	239,145	$5s^25p^2(^3P)6p\ ^2P_{3/2}$	$5s^25p^2(^3P)7s\ ^4P_{1/2}$	4.846×10^6	5.063×10^6	5.461×10^6
1	3031.95	216,141	249,115	$5s^25p^2(^1D)6p\ ^2D_{3/2}$	$5s^25p^2(^3P)6d^4P_{1/2}$	3.455×10^6	1.022×10^6	7.316×10^4
1	3083.27	216,141	248,565	$5s^25p^2(^1D)6p\ ^2D_{3/2}$	$5s^25p^2(^3P)6d^4P_{3/2}$	5.342×10^6	1.452×10^6	2.771×10^5
1	3117.20	219,002	251,073	$5s^25p^2(^1D)4f\ ^2D_{5/2}$	$5s^25p^2(^3P)6d^2F_{7/2}$	7.948×10^7	5.664×10^7	4.145×10^6
4	3143.02	220,082	251,890	$5s^25p^2(^1D)6p\ ^2P_{1/2}$	$5s^25p^2(^3P)6d^2D_{3/2}$	3.672×10^7	4.216×10^6	7.089×10^7
3	3214.51	220,790	251,890	$5s^25p^2(^1D)4f\ ^2P_{1/2}$	$5s^25p^2(^3P)6d^2D_{3/2}$	9.984×10^6	4.387×10^7	2.031×10^6
3	3238.65	215,626	246,494	$5s^25p^2(^1D)6p\ ^2F_{5/2}$	$5s^25p^2(^3P)6d^4D_{7/2}$	1.314×10^5	2.120×10^5	1.061×10^6
1	3241.45	213,736	244,577	$5s^25p^2(^1D)4f\ ^2D_{3/2}$	$5s^25p^2(^3P)6d^4D_{3/2}$	4.030×10^6	4.550×10^6	1.601×10^5
1	3247.11	217,240	248,027	$5s^25p^2(^1D)6p\ ^2F_{7/2}$	$5s^25p^2(^3P)6d^4D_{5/2}$	2.611×10^6	1.551×10^6	2.332×10^5
1	3248.98	235,561	266,331	$5s^25p^2(^1S)6p\ ^2P_{3/2}$	$5s^25p^2(^1D)7s\ ^2D_{5/2}$	2.561×10^6	5.870×10^6	1.354×10^6
2	3515.63	216,141	244,577	$5s^25p^2(^1D)6p\ ^2D_{3/2}$	$5s^25p^2(^3P)6d^4D_{3/2}$	1.258×10^4	8.724×10^1	1.223×10^5
2	3550.01	213,736	241,896	$5s^25p^2(^1D)4f\ ^2D_{3/2}$	$5s^25p^2(^3P)6d^2P_{3/2}$	7.120×10^5	5.240×10^5	1.064×10^6
2	3594.60	216,911	244,722	$5s^25p^2(^1D)6p\ ^2D_{5/2}$	$5s^25p^2(^3P)6d^2F_{5/2}$	8.503×10^5	1.321×10^6	4.517×10^6
1	3636.34	219,002	246,494	$5s^25p^2(^1D)4f\ ^2D_{5/2}$	$5s^25p^2(^3P)6d^4D_{7/2}$	6.194×10^6	3.751×10^6	1.249×10^6
1	3637.66	217,240	244,722	$5s^25p^2(^1D)6p\ ^2F_{7/2}$	$5s^25p^2(^3P)6d^2F_{5/2}$	4.573×10^5	2.214×10^5	1.336×10^6

Table 3. *Cont.*

Int	λ (Å)	Energy (cm^{-1})		Designation		Weighted Transition Rates—gA (s^{-1})		
		Lower	Upper	Lower	Upper	Adjusted		
		Level	Level	Level	Level	HFRa	HFR+CPa	HFR+CP
3	3654.96	224,498	251,851	$5s^25p^2(^1D)6p\ ^2P_{3/2}$	$5s^25p^2(^3P)7s\ ^4P_{5/2}$	3.333×10^5	9.256×10^4	3.850×10^4
2	3715.25	215,626	242,534	$5s^25p^2(^1D)6p\ ^2F_{5/2}$	$5s^25p^2(^3P)6d^4F_{5/2}$	1.159×10^5	1.184×10^4	4.643×10^5
2	3901.70	216,911	242,534	$5s^25p^2(^1D)6p\ ^2D_{5/2}$	$5s^25p^2(^3P)6d^4F_{5/2}$	2.684×10^5	2.945×10^5	3.263×10^4
4	4061.12	224,498	249,115	$5s^25p^2(^1D)6p\ ^2P_{3/2}$	$5s^25p^2(^3P)6d^4P_{1/2}$	9.721×10^5	4.089×10^5	7.330×10^4
3	4248.40	219,002	242,534	$5s^25p^2(^1D)4f\ ^2D_{5/2}$	$5s^25p^2(^3P)6d^4F_{5/2}$	2.127×10^4	6.785×10^4	2.765×10^2
2	4470.40	219,717	242,080	$5s^25p^2(^3P)4f\ ^2F_{7/2}$	$5s^25p^2(^3P)6d^4F_{7/2}$	8.612×10^5	9.968×10^5	1.711×10^4
1	4366.60	219,002	241,896	$5s^25p^2(^1D)4f\ ^2D_{5/2}$	$5s^25p^2(^3P)6d^2P_{3/2}$	4.677×10^5	3.493×10^5	2.294×10^5
1	4505.10	224,498	246,689	$5s^25p^2(^1D)6p\ ^2P_{3/2}$	$5s^25p^2(^3P)7s\ ^4P_{3/2}$	6.198×10^2	2.209×10^4	4.401×10^4
2	4582.85	220,082	241,896	$5s^25p^2(^1D)6p\ ^2P_{1/2}$	$5s^25p^2(^3P)6d^2P_{3/2}$	5.479×10^5	5.230×10^5	5.416×10^4
1	5240.06	232,811	251,890	$5s^25p^2(^1S)6p\ ^2P_{1/2}$	$5s^25p^2(^3P)6d^2D_{3/2}$	1.262×10^6	1.642×10^6	2.573×10^5
4	6348.69	228,975	244,722	$5s^25p^2(^1S)4f\ ^2F_{7/2}$	$5s^25p^2(^3P)6d^2F_{5/2}$	9.962×10^3	9.580×10^3	3.369×10^3

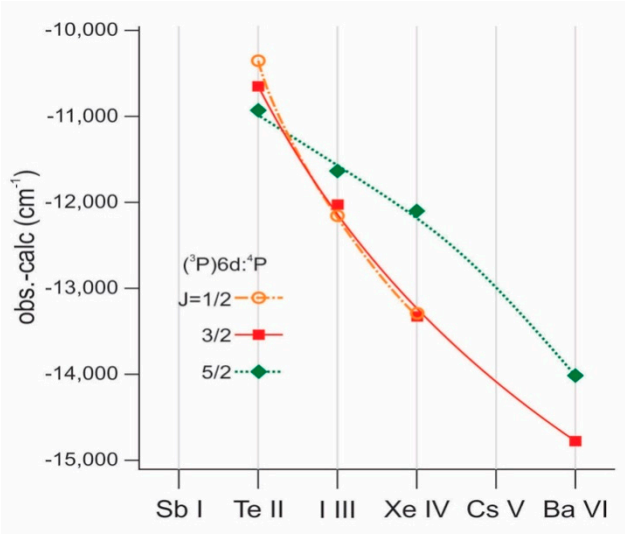

Figure 2. Isoelectronic trend for the multiplet (^{3}P) ^{4}P energy levels of the 5s^{2}5p^2 6d configuration.

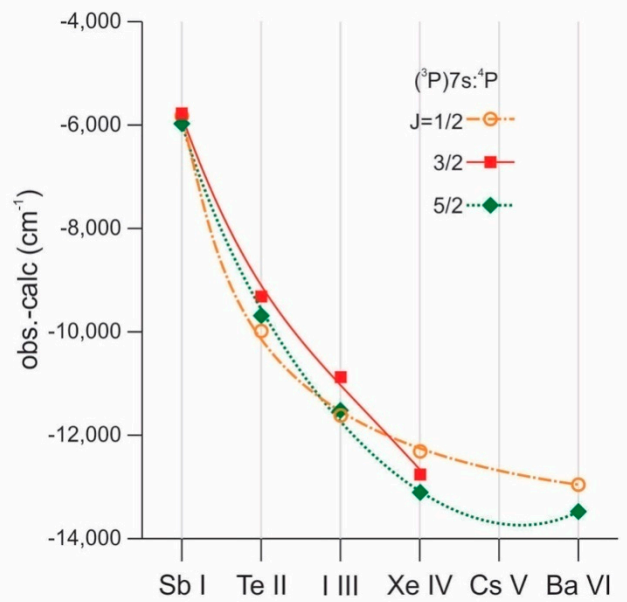

Figure 3. Isoelectronic trend for the multiplet (^{3}P) ^{4}P energy levels of the 5s^{2}5p^2 7s configuration.

Table 4 shows the result of least squares adjustment for even parity levels, where 6d and 7s configurations are included. All single configuration parameters, the R^k integrals for 5s5p^4-5s^{2}5p^{2}6s, 5s5p^4-5s^{2}5p^{2}5d, 5s^{2}5p^{2}6s-5s^{2}5p^2 5d interactions, and the R^1(5p,5d;6d,5p)of the 5s^{2}5p^2 5d-5s^{2}5p^{2}6d interaction were left free during the final calculation. The rest of the configuration interaction integrals remained fixed at 85% of their Hartree–Fock values. We found a standard deviation of 138 cm^{-1} for this adjustment.

Table 4. Least-squares parameters for even parity of Xe IV. Standard deviation is 138 cm^{-1}.

Configuration	Parameter	HFR (cm^{-1})		HFRa./HFR [a]
		HFR	HFRa	
$5s5p^4$	$E_{av}(5s5p^4)$	145,275	132,757	−12,519
	$F^2(5p,5p)$	53,464	46,502	87%
	α	0	−402	
	ζ_{5p}	8246	8600	104%
	$G^1(5s,5p)$	70,216	48,430	69%
$5s^25p^26s$	E_{av} $(5s^25p^26s)$	187,245	176,036	−11,209
	$F^2(5p,5p)$	54,783	43,692	80%
	α	0	−55	
	ζ_{5p}	8859	8945	101%
	$G^1(5p,6s)$	5898	4379	74%
$5s^25p^27s$	E_{av} $(5s^25p^27s)$	267,957	257,041	−10,916
	$F^2(5p,5p)$	55,283	47,384	86%
	ζ_{5p}	8999	8556	95%
	$G^1(5p,7s)$	1801	1633	91%
$5s^25p^25d$	E_{av} $(5s^25p^25d)$	170,438	158,790	−11,648
	$F^2(5p,5p)$	54,191	42,089	78%
	α	0	−123	
	ζ_{5p}	8593	8754	102%
	ζ_{5d}	478	695	145%
	$F^2(5p,5d)$	39,705	32,721	82%
	$G^1(5p,5d)$	44,921	32,124	72%
	$G^3(5p,5d)$	28,247	20,111	71%
$5s^25p^26d$	E_{av} $(5s^25p^26d)$	264,034	253,060	−10,975
	$F^2(5p,5p)$	55,267	47,585	86%
	ζ_{5p}	8972	8449	94%
	ζ_{6d}	161	153	95%
	$F^2(5p,6d)$	11,723	10,009	85%
	$G^1(5p,6d)$	7747	6753	87%
	$G^3(5p,6d)$	5444	5575	102%
$5s5p^4$-$5s^25p^26s$	$R^1(5p,5p;5s,6s)$	−1237	−851	69%
$5s5p^4$-$5s^25p^27s$	$R^1(5p,5p;5s,7s)$	−1351	−1148	85%
$5s5p^4$-$5s^25p^25d$	$R^1(5p,5p;5s,5d)$	53,926	37,094	69%
$5s5p^4$-$5s^25p^26d$	$R^1(5p,5p;5s,6d)$	22,435	19,069	85%
$5s^25p^26s$-$5s^25p^27s$	$R^1(5p,6s;7s,5p)$	3120	2652	85%
$5s^25p^26s$-$5s^25p^25d$	$R^2(5p,6s;5p,5d)$	−12,799	−10,336	81%
	$R^1(5p,6s;5d,5p)$	−5075	−4098	81%
$5s^25p^26s$-$5s^25p^26d$	$R^2(5p,6s;5p,6d)$	4779	4062	85%
	$R^1(5p,6s;6d,5p)$	85	73	85%
$5s^25p^27s$-$5s^25p^25d$	$R^2(5p,7s;5p,5d)$	−6519	−5541	85%
	$R^1(5p,7s;5d,5p)$	−3294	−2800	85%
$5s^25p^27s$-$5s^25p^26d$	$R^2(5p,7s;5p,6d)$	−3058	−2599	85%
	$R^1(5p,7s;6d,5p)$	−391	−333	85%
$5s^25p^25d$-$5s^25p^26d$	$R^2(5p,5d;5p,6d)$	12,162	10,338	85%
	$R^1(5p,5d;6d,5p)$	17,415	13,061	75%
	$R^3(5p,5d;6d,5p)$	11,432	9717	85%

[a] Ratio HFRa to HFR for each case, except for average energies, where values are the difference of HFRa minus HFR for each case.

4. Conclusions

In this study we extended the knowledge of the Xe IV spectrum to the $5s^25p^27s$ and $5s^25p^2$ 6d configuration, from a set of 163 new line classifications. To produce this new information, we used a

set of different analysis tools, including calculations from three models (HFR, HFR+CP, and MCDF), least-squares adjustment, line intensity comparisons, and isoelectronic analysis, which makes us very confident in our results.

Author Contributions: All authors contributed equally to this work.

Funding: This research received no external funding.

Acknowledgments: This research was supported by the Consejo Nacional de Investigaciones Científicas y Tecnicas (CONICET), Argentina, and by the Coordenação de Aperfeiçoamento de Pessoal de Nível Superior (CAPES), Brazil, Finance Code 001. The authors thank Espaço da Escrita–Pró-Reitoria de Pesquisa–UNICAMP-for the language services provided. Support of the Comision de Investigaciones Científicas de la Província de Buenos Aires (CIC), where M.R. is a researcher, is also gratefully acknowledged.

Conflicts of Interest: The authors declare no conflicts of interest.

References

1. Gustafsson, B. The future of stellar spectroscopy and its dependence on YOU. *Phys. Scr.* **1991**, *34*, 14–19. [CrossRef]
2. Biémont, E.; Blagoev, K.; Campos, J.; Mayo, R.; Malcheva, G.; Ortíz, M.; Quinet, P. Radiative parameters for some transitions in Cu(II) and Ag(II) spectrum. *Spectrosc. Relat. Phenom.* **2005**, *144*, 27–28. [CrossRef]
3. Cowley, C.R.; Hubrig, S.; Palmeri, P.; Quinet, P.; Biémont, É.; Wahlgren, G.M.; Schütz, O.; González, J.F. HD 65949: Rosetta stone or red herring. *Mon. Not. R. Astron. Soc.* **2010**, *405*, 1271–1284. [CrossRef]
4. Otsuka, M.; Tajitsu, A. Chemical abundances in the extremely carbon-rich and xenon-rich halo planetary nebula H4-1. *Astrophys. J.* **2013**, *778*, 146. [CrossRef]
5. Péquignot, D.; Baluteau, J.-P. The identification of krypton, xenon, and other elements of rows 4, 5 and 6 of the periodic table in the planetary nebula NGC 7027. *Astron. Astrophys.* **1994**, *283*, 593–625.
6. Biémont, E.; Hansen, J.E.; Quinet, P.; Zeippen, C.J. Forbidden transitions of astrophysical interest in the 5pk (k=1–5) *configurations*. *Astron. Astrophys. Suppl. Ser.* **1995**, *111*, 333–346.
7. Werner, K.; Rauch, T.; Ringat, E.; Kruk, J.W. First detection of krypton and xenon in a white dwarf. *Astrophys. J.* **2012**, *753*, L7. [CrossRef]
8. Rauch, T.; Hoyer, D.; Quinet, P.; Gallardo, M.; Raineri, M. The Xe VI ultraviolet spectrum and the xenon abundance in the hot do-type white dwarf RE 0503−289. *Astron. Astrophys.* **2015**, *577*, A88. [CrossRef]
9. Zhang, Y.; Liu, X.-W.; Luo, S.-G.; Péquignot, D.; Barlow, M.J. Integrated spectrum of the planetary nebula NGC 7027. *Astron. Astrophys.* **2005**, *442*, 249–262. [CrossRef]
10. Zhang, Y.; Williams, R.; Pellegrini, E.; Cavagnolo, K.; Baldwin, J.A.; Sharpee, B.; Phillips, M.; Liu, X.-W. Abundances of s-process elements in planetary nebulae: Br, Kr &Xe in Planetary Nebulae in Our Galaxy and Beyond. *Proc. IAU Symp.* **2006**, *234*, 549–550. [CrossRef]
11. Saloman, E.B. Energy levels and observed spectral lines of xenon, Xe I through Xe LIV. *J. Phys. Chem. Ref. Data* **2004**, *33*, 765–921. [CrossRef]
12. Gallardo, M.; ReynaAlmandos, J.G. *XenonLines in the Range from 2000 Å to 7000 Å*; Serie "Monografias Cientificas" No. 1; Centro de Investigaciones Opticas: LaPlata, Argentina, 1981.
13. Tauheed, A.; Joshi, Y.N.; Pinnington, E.H. Revised and extended analysis of the $5s^25p^3$, $5s5p^4$, $5s^25p^25d$ and $5s^25p^26s$ configurations of trebly ionized xenon (Xe IV). *Phys. Scr.* **1993**, *47*, 555–560. [CrossRef]
14. Gallardo, M.; Raineri, M.; Reyna Almandos, J.G.; Di Rocco, H.O.; Bertuccelli, D.; Trigueiros, A.G. 5s25p2(6p + 4f) configurations in triply ionized xenon (Xe IV). *Phys. Scr.* **1995**, *51*, 737–751. [CrossRef]
15. Raineri, M.; Lagorio, C.; Padilla, S.; Gallardo, M.; Reyna Almandos, J. Weighted oscillator strengths for the Xe IV spectrum. *At. Data Nucl. Data Tables* **2008**, *94*, 140–159. [CrossRef]
16. Bertuccelli, G.; Di Rocco, H.O.; Iriarte, D.I.; Pomarico, J.A. Experimental Determination of Transition Probabilities of Xe IV; Comparison with Semiempirical Calculations. *Phys. Scr.* **2000**, *62*, 277–281. [CrossRef]
17. Cowan, R.D. *The Theory of Atomic Structure and Spectra*; University of California Press: Berkeley, CA, USA, 1981.
18. Pagan, C.J.B.; Raineri, M.; Gallardo, M.; Reyna Almandos, J. Spectral Analysis and New Visible and Ultraviolet Lines of ArV. *Astron. Astrophys. Suppl. Ser.* **2019**, *242*, 24. [CrossRef]

19. Dyal, K.G.; Grant, I.; Johnson, C.T.; Parpia, F.A.; Plummer, E.P. GRASP: A general-purpose relativistic atomic structure program. *Comput. Phys. Commun.* **1989**, *55*, 425–456. [CrossRef]
20. Reyna Almandos, J.; Bredice, F.; Raineri, M.; Gallardo, M. Spectral analysis of ionized noble gases and implications for astronomy and laser studies. *Phys. Scr.* **2009**, *T134*, 014018. [CrossRef]
21. Raineri, M.; Gallardo, M.; Pagan, C.J.B.; Trigueiros, A.G.; ReynaAlmandos, J. Lifetimes and transition probabilities in KrV. *J. Quant. Spectrosc. Radiat. Transf.* **2012**, *113*, 1612–1627. [CrossRef]
22. Quinet, P.; Palmeri, P.; Biémont, E.; McCurdy, M.M.; Rieger, G.; Pinnington, E.H.; Wickliffe, M.E.; Lawler, J.E. Experimental and theoretical radiative lifetimes, branching fractions and oscillator strengths in Lu II. *Mon. Not. R. Astron. Soc.* **1999**, *307*, 934–940. [CrossRef]
23. Koch, V.; Andrae, D. Static Electric DipolePolarizabilities for Isoelectronic Sequences. *Int. J. Quantum Chem.* **2011**, *111*, 891–903. [CrossRef]
24. Grant, I. *Relativistic Quantum Theory of Atoms and Molecules: Theory and Computation*; Springer: Oxford, UK, 2007.
25. Kramida, A. Configuration interactions of class 11: Na error in Cowan's atomic structure theory. *Comput. Phys.Commun.* **2017**, *215*, 47–48. [CrossRef]
26. Kramida, A. Corrigendum to "Configuration interactions of class 11: Na error in Cowan's atomic structure theory". *Comput. Phys. Commun.* **2018**, *232*, 266–267. [CrossRef]
27. NIST Standard Reference Database 78. Version 5.6. Available online: https://www.nist.gov/pml/atomic-spectra-database (accessed on 31 October 2018).
28. Sharman, M.K.; Tauheed, A.; Rahimullah, K. Spectral analysis of $5s^2 5p^2$ (6p+6d+7s) configurations of Ba VI. *J. Quant. Spectrosc. Radiat. Transf.* **2014**, *142*, 37–48. [CrossRef]

© 2019 by the authors. Licensee MDPI, Basel, Switzerland. This article is an open access article distributed under the terms and conditions of the Creative Commons Attribution (CC BY) license (http://creativecommons.org/licenses/by/4.0/).